Biochimica et Biophysica Acta 1818 (2012) 2927–2935

Contents lists available at SciVerse ScienceDirect

Biochimica et Biophysica Acta

journal homepage: www.elsevier.com/locate/bbamem

Efficacy verification and microscopic observations of an anticancer peptide, CB1a, on single lung cancer cell

Feng-Sheng Kao [a,b], Yun-Ru Pan [a], Ray-Quen Hsu [b], Hueih-Min Chen [a,*]

[a] National Nano Device Laboratories, Nano Biomedical Group, Hsinchu, Taiwan
[b] National Chiao Tung University, Department of Mechanical Engineering, Hsinchu, Taiwan

ARTICLE INFO

Article history:
Received 22 March 2012
Received in revised form 20 July 2012
Accepted 23 July 2012
Available online 28 July 2012

Keywords:
Atomic force microscopy
CB1a, single cell
Cancer cell
Anticancer peptide

ABSTRACT

In this work, we introduce a new customized anti-lung cancer peptide, CB1a, with IC_{50} of about 25.0 ± 1.6 μM on NCI-H460 lung cancer cells. Using a multi-cellular tumor spheroid (MCTS) model, results show that CB1a is potent in preventing the growth of lung cancer tumor-like growths *in vitro*. Additionally, atomic force microscopy (AFM) was used to examine cell surface damage of a single cancer. The mechanism for cell death under CB1a toxicity was verified as being largely due to cell surface damage. Moreover, with a treatment dosage of CB1a at 25 μM, Young's module (E) shows that the elasticity and stiffness of cancer cell decreased with time such that the interaction time for a 50% reduction of E (IT_{50}) was about 7.0 min. This new single-cell toxicity investigation using IT_{50} under AFM assay can be used to separately verify drug efficacy in support of the traditional IC_{50} measurement in bulk solution. These results could be of special interest to researchers engaged in new drug development.

1. Introduction

As natural antibiotics, most antimicrobial peptides (AMPs) have both cationic and amphipathic properties that allow them to interact with bacterial cytoplasmic membranes leading to cell death [1–4]. Mutation of these natural AMPs can significantly alter bacterial killing ability. For example, a recent study showed that N-acylated mutant of LF11 derived from human latoferricin could enhance antimicrobial activity on *Escherichia coli* [5]. Some AMPs such as cecropins [6–8], magainins [9–14], melittins [15–17], human LL-37 [18–23] and host defense peptides [24,25] have the ability to kill cancer cells. Both cell-killing mechanisms (antimicrobial and anticancer) may share similarities such as membranolysis [26–30]. Among these peptides, melittin is the most toxic to human cells. However, a recent report [31] showed that if melittin was used to form complexes with nanoparticles, its anti-cancer ability could be enhanced, half-life increased, and toxicity in mice decreased. These observations imply that under particular circumstances altering original peptides can make them more effective in killing cells [30].

Cecropins (such as cecropins A, B, C, D, E and F) belong to a family of natural antimicrobial peptides composed of 34–39 amino acids of high sequence homology [7,32]. These peptides have common characteristics. They are mostly constructed with α-helical structure at the amphipathic N-terminal (where one side is hydrophilic and the other hydrophobic) and the hydrophobic residues of the C-terminal. Cecropin B (CB) has the strongest antibacterial activity of this family. Our previous studies have shown that CB can disrupt bacterial membranes and also kill cancer cells including leukemia, stomach carcinoma, and lung cancer cells [33–38]. However, the efficacies of CB on killing cancer cells were not as good as for killing bacteria as compared with other anti-cancer agents. The possible explanation is that CB which is naturally good to kill bacteria may not be good to apply it for killing such as cancer cells where the surface conformations are different from bacteria's. For the purpose of developing an effective anti-cancer peptide, therefore, a new design using natural CB's sequence as a template is essential. Accordingly, peptide, CB1a, was constructed by using three-repeated amphiphathic section of the CB N-terminal (Lys-Trp-Lys-Val-Phe-Lys-Lys-Ile-Glu-Lys or KWKVFKKIEK) and bridged with Ala-Gly-Pro (or AGP) as: NH_2-KWKVFKKIEK-KWKVFKKIEK-AGP-KWKVFKKIEK-COOH (see Ref. [39] for details). Nuclear Magnetic Resonance (NMR) structural study showed that CB1a has two helices kinked (kink angle: 110°) by a bridge, Ala-Gly-Pro (see RCSB-Protein Data Bank; 2IGR). The advantages in creating CB1a as a custom anticancer peptide were: (i) Proline involved in the bridge or kink section as it can be effectively used for oligomerization and pore gating in the lipid bilayer of cancer cell membranes [40,41]; (ii) The three repeated amphipathic sections of CB1a allow for high flexibility to dynamically pass through the cell surface to the cell lipid bilayer; (iii) The high density of positive charge (net +12) which provides strong binding capacity with cancer cell membranes, which have a high negative

Abbreviations: AFM, atomic force microscopy; AMP, antimicrobial peptide; CB, cecropin B; Dox, doxorubicin; EM, electron microscopy; IT_{50}, interaction time (IT) for reducing 50% of E; MCTS, Multi-cellular tumor spheroids; SI, selectivity index; SOP, standard operation procedure

* Corresponding author at: National Nano Device Laboratories, Nano Biomedical Group, No. 26, Prosperity Road I, Hsinchu Science Park, Hsinchu, 30078, Taiwan. Tel.: +886 3 5726100×7712.
E-mail address: hmchen@ndl.narl.org.tw (H.-M. Chen).

0005-2736/$ – see front matter © 2012 Elsevier B.V. All rights reserved.
http://dx.doi.org/10.1016/j.bbamem.2012.07.019

charge due to lipids [30]. Consequently, the customized peptide CB1a met both the selectivity and toxicity criteria for killing cancer cells [39].

Since CB1a likely kills cancer cells in a similar way as the AMPs mentioned above i.e., through lipid corruption at the membrane, the method is described as a physical rather than chemical attack. Chemical attacks describe inhibition of chemical reactions at binding sites inside the cell such as those for RNA and DNA. To measure the physical changes in cancer-cell surfaces before and after physical attack by CB1a, both the elastic force and morphological changes of the cell membrane were analyzed by atomic force microscopy (AFM). Comparisons of stiffness between cancer and normal cells *via* AFM measurements have been previously reported and confirmed in terms of clinical concerns about the stiffness of cells, which varies according to the different mechanical characteristics of membranes [42–48]. Most recently, mechanical stiffness has been correlated with the plasma membrane potential of vascular endothelial cell using a combination of fluorescence-based membrane potential recording and AFM-based stiffness measurements [49]. Unlike electron microscopy, AFM does not require any additional cell-preparation treatments and samples can be imaged under nearly native conditions with minimal alteration or damage. Additionally, AFM allows for real-time observation of cell morphological changes.

In this study, we verify the efficacy of CB1a on lung cancer cells in bulk solution using half maximal inhibitory concentration (IC_{50}) by 3-(4,5-dimethylthiazol-2-yl)-2,5-diphenyl tetrazolium bromide (MTT) assay. A multi-cellular tumor spheroid (MCTS) model in test tubes is also applied to show that CB1a is potent in preventing the growth of lung cancer tumor-like growths. Furthermore, we identify the killing pathway for a single cancer cell by observing damage to the cell surface under AFM measurements. Results show that CB1a has high selectivity for cancer cells over normal lung cells. While, doxorubicin (Dox) currently used in clinics does not have high selectivity and causes damage to both normal lung and cancer cells, which can lead to serious side effects in patients. Since CB1a has both low toxicity and high selectivity, it may make a good candidate for further development as an anti-cancer drug.

2. Materials and methods

2.1. Materials

The AFM tip (pointprobe®) was purchased from Nanosensor (Switzerland). Micro-particle (diameter ~10 μm) was obtained from Bangs Laboratories (USA). Cell culture media, fetal bovine serum (FBS) and antibiotics—penicillin and streptomycin were purchased from Gibco (USA). RPMI-1640 medium, hydrochloride acid, sodium bicarbonate and 3-(4,5-dimethylthiazol-2-yl)-2,5-diphenyl tetrazolium bromide (MTT) were obtained from Sigma (USA). Doxorubicin was purchased from Pfizer (Italy). Cancer cell lines NCI-H460/NCI-H520 and fibroblast cell line MRC-5 were purchased from the American Type Culture Collection (ATCC; USA). Water used was de-ionized and distilled.

2.2. Preparation of peptides

Both CB1a and CB peptides were solid-phase synthesized by peptide synthesizer (Applied Biosystem Inc.) [50]. Fmoc (9-fluorenylmethyloxycarbonyl) and HBTU (O-benzotriazole-N,N,N′, N′-tetramethyl-uronium-hexafluoro-phosphate)/HOBT (N- hydroxybenzotriazole) were used as protection and coupling reagents, respectively. Final products were de-protected and cleaved from the peptide resin using a solution containing tri-fluoroacetic acid (TFA), water, phenol, thioanisole and ethanedithiol. The remaining resin was removed by filtration and the peptides precipitated with diethyl ether after the organic solvents had evaporated. The crude peptides were desalted on Sephadex G-10 (20% acetic acid) and purified by reverse phase high pressure liquid chromatography (HPLC) (Vydac C-18 column, 0.1% TFA in H_2O-acetonitrile). Product purities were determined by HPLC and found to be 95% and 96% for CB1a and CB, respectively. Molecular weights (MWs) of the peptides were determined by mass spectrometry and found to be almost identical to the theoretical values (Both observed/calculated MWs (g/mol) are 4191.2/4190.3 and 3834.8/3836.0 for CB1a and CB, respectively). Concentrations of peptides were determined from the net weight of peptides and their molecular masses (the weight of associated counter ions was not taken into consideration).

2.3. Cell culture and cytotoxicity assays

Lung cancer cell lines (NCI-H460 and NCI-H520) were grown in RPMI-1640 culture media supplemented with 10% FBS and 1% penicillin–streptomycin (PS) antibiotic mixture. Lung fibroblast cell line (MRC-5) was cultured in MEM medium containing 10% FBS and 1% PS mixture. The above cell lines were cultured at 37 °C in a 5% CO_2 humidified incubator.

The cell suspensions were adjusted to contain 1×10^5 cells/ml before they were transferred into a 96-well plate (90 μl/well). Each well was then mixed with 10 μl of peptide solution of different concentrations (0, 1, 5, 10, 15, 20, 30, 50, 100 and 200 μM) and each sample collected in triplicate. After 24 h incubation, a MTT-based colorimetric assay was conducted by adding 40 μl MTT (2 mg/ml)/100 μl DMSO into each well at room temperature for 10 min (MTT can be metabolized by mitochondrial de-hydrogenases in metabolically active cells to form a formazan salt with strong absorption at 570 nm ($A_{570\ nm}$)). $A_{570\ nm}$ of each well sample was measured using a Bio-Rad model 450 microtiter plate reader. Cell survival rate (%) was determined by $(\Delta A_{570\ nm}/A'_{570\ nm})\times100$, where $\Delta A_{570\ nm}=A''_{570\ nm}-A'_{570\ nm}$, $A'_{570\ nm}$ is the sample's absorbance without addition of peptide, and $A''_{570\ nm}$ is sample's absorbance with the addition of peptide. IC_{50} (half maximal inhibitory concentration) was obtained from the plot of survival rates (%) *vs.* peptide concentrations. An illustration of IC_{50} measurement for CB1a at different batch productions (CB1a_1 and CB1a_2) is shown in Fig. 1.

2.4. Multi-cellular tumor spheroid culture

Multi-cellular tumor spheroids (MCTS) of NCI-H460 cancer cells were constructed on non-adhesive, bacterial culture-grade polystyrene

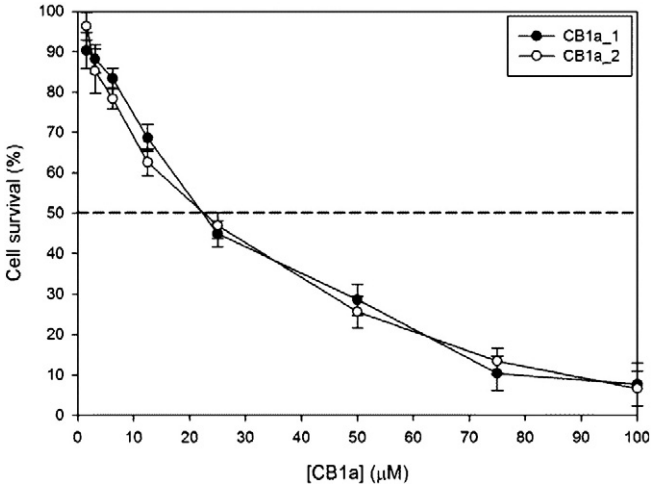

Fig. 1. IC_{50} measurements of CB1a on lung cancer cell line, NCI-H520. Two measurements were done (CB1a peptides were produced by different batches, CB1a_1 and CB1a_2, respectively). IC_{50} of CB1a was about 25.0 ± 1.6 μM. Each point was the average of five experimental measurements.

Petri dishes using a modified hanging drop method [51]. Approximately, 500 single cells at a density of 3×10^4 cells/ml were deposited as drops on the lids of 90-mm Petri dishes to generate cellular aggregates. Lids with droplets attached were inverted over dishes filled with 10-ml PBS and incubated at 37 °C in a 5% CO_2 incubator. NCI-H460 cancer cells were de-attached and MCTS were then obtained: (i) without CB1a treatment; (ii) with immediate CB1a treatment; (iii) post 30 min of CB1a treatment.

2.5. Cell images

Cell (NCI-H460 lung cancer cell and MRC-5 normal lung cell) damage induced by CB1a was observed by AFM (NanoWizard BioAFM, JPK, Germany) at a resolution of 512×512 pixels. A silicon-made AFM tip (NanoWorld, Switzerland) with a spring constant of 0.02 N/m was used for cell surface imaging measurement. After drug (CB1a or Dox) treatment, the medium was removed and the remaining sample washed by 1× PBS solution at pH 7.2. The desired cell was then fixed by 4% paraformaldehyde at room temperature for 10 min. The sample was rinsed again by 1X PBS buffer, water, and then air dried. The details of the set-up procedures for AFM to obtain cell morphology or mechanical property changes are shown in Appendix. Typical examples of "single cell" images (topology image and 3D configuration) by AFM tip are shown in Fig. 2.

2.6. Young's modulus (E) measurement

A polystyrene bead (diameter ~10 μm) was attached to the AFM tip by epoxy resin. The spring constant (0.04 N/m) of the bead-attached cantilever was calibrated in the cell culture medium by force modulation mode. All experiments were done within 30 min to insure living cells. Young's modulus, E, on the cell was determined by fitting a simplified parabolic geometric equation [52]:

$$F = \frac{4\sqrt{R}}{3}\frac{E}{1-\nu^2}\delta^{\frac{3}{2}} \quad (1)$$

where F is an applied external force, R is radius of tip, δ is the indentation depth of sample, which can be calculated by $\delta = h - d$, where h is an indented piezo height and d is distance of cantilever's deflection. ν is Poisson's ratio (0.5 was used for soft biological sample). E is Young's modulus obtained after fitting with F vs. δ curve. An illustration of obtaining E on a single cancer cell after treatment with CB1a is shown in Fig. 3 (fitting curves are shown in bold). In these examples, Es were 760 pa and 119 pa for tip interaction time with the cell surface at 5 min and 19 min, respectively. Detailed results are given in the "Results" section below.

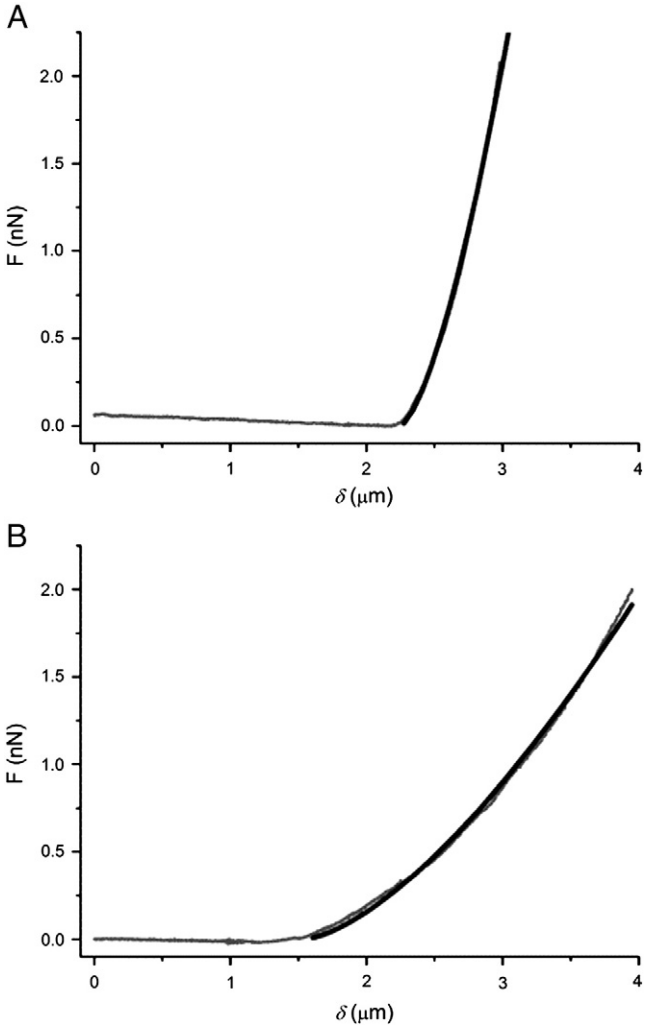

Fig. 3. Calculation of E. Typical examples of F vs. δ for single cancer cell (NCI-H460) treated with CB1a (25 μM) were shown at time (A) 5 min and (B) 19 min after AFM tip approached the cell surface. Fitting lines are shown in bold.

3. Results

3.1. Anti-cancer activity assays and multi-cellular tumor spheroids

Cytotoxicity assays of agents including CB, CB1a and Dox were done on lung cancer and normal lung cells. IC_{50}s of these compounds

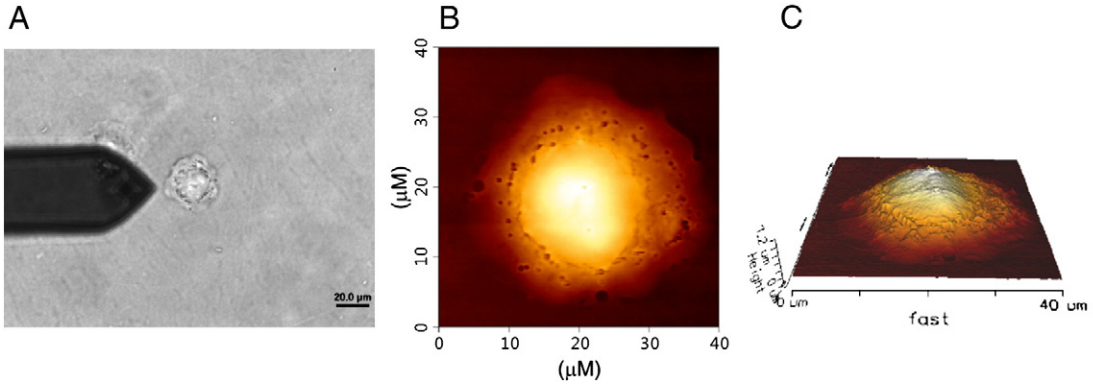

Fig. 2. Typical AFM morphological observations for single cancer cell. (A) AFM tip approaches cancer cell; (B) cell topology image; (C) cell 3D configuration. X- and Y-axis are for the dimensions of "width" and "length" of cell and the scale shown in the corner between X- and Y-axis indicates the "height" of cell. For NCI-H460 cell, the dimension confined in AFM output is 40 (width)×40 (length) μm with height of 0–1.2 μm.

Table 1
IC_{50s} of CB, CB1a and DOX on lung cancer and normal lung cells.

IC_{50} (μM)	Lung cancer cells		Normal lung cell
	NCI-H460	NCI-H520	MRC-5
CB	>200	58.8 ± 2.0	>100
CB1a	25.0 ± 1.6	22.7 ± 1.2	>100
Dox	18.4 ± 0.8	18.0 ± 1.0	16.6 ± 1.4

are shown in Table 1. As compared with CB, CB1a has lower IC_{50}s on lung cancer cells (25.0 ± 1.6 μM for NCI-H460 and IC_{50} = 22.7 ± 1.2 μM for NCI-H520) and equally higher IC_{50} on normal lung cells (IC_{50} > 100 μM for MRC-5). This implies that CB1a is outstandingly cytotoxic to lung cancer cells while not being seriously harmful to normal lung cells. For Dox, although it has lower IC_{50}s on both lung cancer cell lines (18.4 ± 0.8 μM and 18.0 ± 1.0 μM for NCI-H460 and NCI-H520, respectively), the IC_{50} on normal lung cells is even lower (only 16.6 ± 1.4 μM for MRC-5). In other words, Dox is more toxic to normal lung cells than abnormal cells with the potential for causing serious side-effects in cancer patients. Compared with Dox, CB1a seems to have much higher selectivity for lung cancer cells over normal lung cells.

In addition to *in vitro* toxicity testing of CB1a on cancer and normal cells above, further efficacy investigation of this peptide on cancer cell-aggregated tumor-like growths was identified by *ex vivo* MCTS modeling. In this case, NCI-H460 cancer cells were de-attached and MCTS were then obtained: (i) without CB1a treatment; (ii) with immediate CB1a treatment; (iii) post 30 min of CB1a treatment. Fig. 4A to C shows the respective results of the three different tumor growth scenarios. In Fig. 4A, a complete solid tumor-like growth formed when NCI-H460 cancer cells were added into a test tube. Fig. 4B shows a degraded tumor if CB1a peptide was added simultaneously to the test tube along with the cancer cells. Fig. 4C shows that only small spots formed in the test tube if CB1a peptide was added 30 min in advance of cell seeding. This result indicates that CB1a damages cancer cells and prevents cell–cell interaction/aggregation and consequently interrupts tumor-like growth.

3.2. AFM observations for single normal lung cell, MRC-5, treated with CB1a and Dox

(1) CB1a effect: AFM 3D images of single normal lung cell, MRC-5, under CB1a (25 μM) treatment at time 0, 0.5, 2, 8, 16 and 24 h are shown in Fig. 5A to F, respectively. For different incubation times, the cell nucleus (raised area in white) can be seen in each figure. This is consistent with no significant morphological change, indicating MRC-5 remained healthy for the times of the experiment; i.e., CB1a did not cause obvious injury to a normal lung cell during the 24 h test period.

(2) Dox effect: Healthy MRC-5 cell was observed after dosing with 18 μM Dox at 2 h; 8 h; 16 h and 24 h and the results shown in Fig. 6A to D. By 8 h the cell had become flatter, by 16 h the cell nucleus had begun to breakdown and by 24 h the cell had completely collapsed. These results show that Dox is toxic to a normal lung cell within 8 h.

3.3. AFM observations for single lung cancer cell treated with CB1a

Cytotoxicity effects of CB1a on single human lung cancer cells, NCI-H460 and NCI-H520, were done by AFM observations. A cellular surface image of NCI-H460 without CB1a treatment is shown in Fig. 7A. The cell shape is smooth and round (diameter ~35 μm) and it has a distinctive contour marking the nucleus. A similar observation for NCI-H520 without treatment with CB1a was obtained (see Fig. 7D). Treatments with CB1a at different concentrations of 25 and 50 μM were done on two cell lines for 30 min. Results show that these single cells became sunken and appeared to have irregular shapes or ragged cellular configurations (see Fig. 7B and C for NCI-H460 and Fig. 7E and F for NCI-H520). These results indicate CB1a is highly toxic to cancer cells within 30 min.

3.4. Single cell surface damage determined by Young's modulus (E)

The physical changes in the properties of cell surface induced by CB1a are given by real-time measurement of *E* for a CB1a-treated single cell. Plots of normalized Young's modulus *E vs.* time are shown in Fig. 8. Without CB1a treatment, *E* of NCI-H460 cell remained at about 1.0 (Fig. 8A) within 25 min. After the addition of 12.5 μM CB1a, the level of *E* gradually declined to about 0.62 by 30 min (Fig. 8B). These results indicate CB1a's effects on cell surface. However, the shape of the line is still similar to that of Fig. 8A; i.e., almost flat. The shape of the *E* line *vs.* time changes when the concentration of CB1a's increases to 25 μM. This result is similar to that of IC_{50} (see Fig. 1). *E* drops in a reverse parabolic contour to about only 35% within 10 min. To give the expression of *E* physical meaning, a new term IT_{50} is defined in this work. It indicates interaction time (IT) whereby *E* is reduced by 50%. Accordingly, IT_{50}s of CB1a on NCI-H460 were 7.0 min at 25 μM (see Fig. 8C) and 4.8 min at 50 μM (see Fig. 8D). Furthermore, *E* for CB1a-treated MRC-5 normal lung cell was also investigated. Plots of normalized *E vs.* time for CB1a at 5 and 25 μM are shown in Fig. 9A

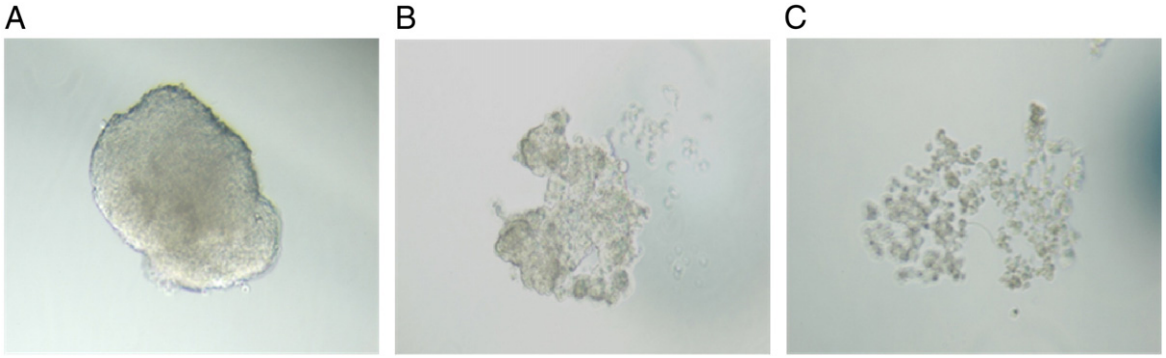

Fig. 4. Spheroidal tumor-like growth formed by NCI-H460 cancer cells in test tube. (A) tumor formed without addition of CB1a; (B) tumor formed with simultaneous addition of CB1; (C) tumor formed with pre-addition of CB1a by 30 min. Concentration of CB1a was 25 μM and initial cancer cell concentration was 2×10^3 cells. All photos were taken after 24 h.

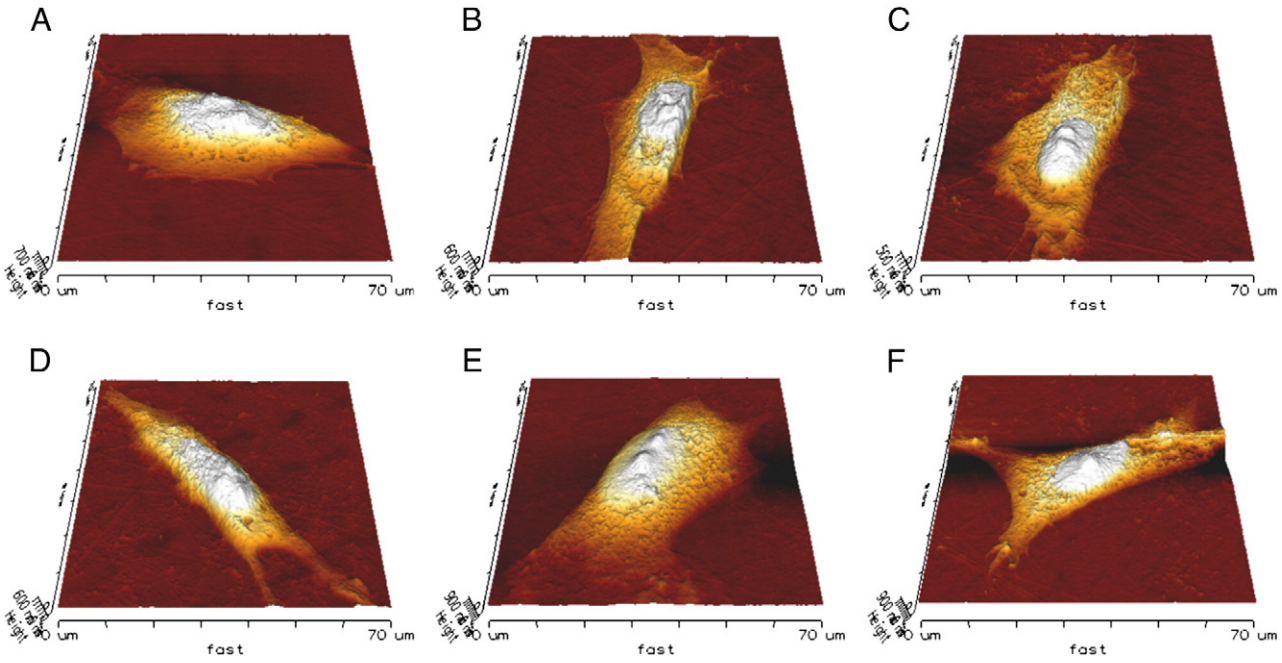

Fig. 5. AFM images of MRC-5 cell treated with CB1a (25 μM) at (A) 0 h; (B) 0.5 h; (C) 2 h; (D) 8 h; (E) 16 h and (F) 24 h. Since both cellular size and shape of MRC-5 cell are irregular, a fixed area (70×70 μm) was confined and detected. The raised area in white in each figure is about 12 μm in width and 20–25 μm in length.

and B, respectively. Both *E*s were more or less constant (at around 1.0) and IT_{50}s were infinite. These results indicate no changes to the physical condition of the normal lung cell under treatment with CB1a at 25 μM within 30 min.

4. Discussion

Therapeutic drugs work via chemical or physical pathways in the treatment of cancer cells. A physical attack on a cancer cell is one where cellular membranes are compromised leading to cell death. Understanding the mechanism of cellular death is essential for the development of peptides as anticancer drugs. This paper investigates a customized peptide from the CB group, CB1a, to see how cell damage occurs in a single cell by AFM microscopic observations and test the efficacy and selectivity of CB1a against lung cancer cells. Before the single cell measurements, general investigations of IC_{50} for CB1a on lung cancer and normal lung cells *via* MTT assay were performed. We used the current clinically available drug, Dox, as a reference compound. Based on the results of MTT assay, CB1a has high selectivity for lung cancer cells over normal cells. Its selectivity was much better than

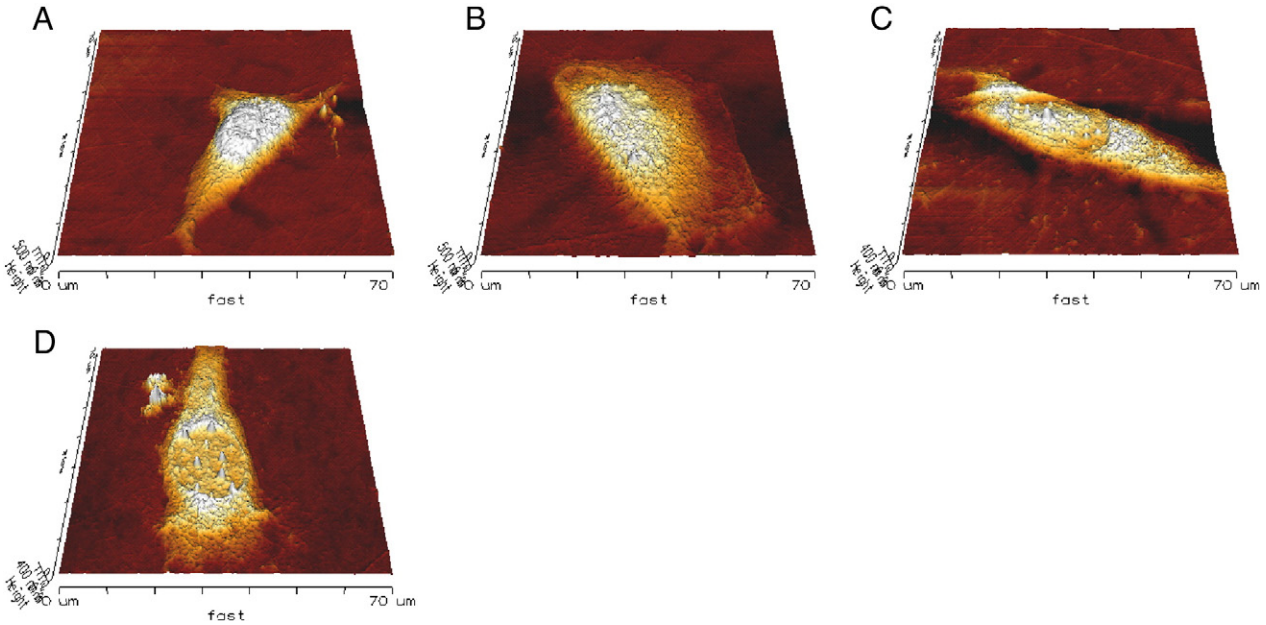

Fig. 6. AFM images (70×70 μm) of MRC-5 treated with Dox (18 μM) at (A) 2 h; (B) 8 h; (C) 16 h and (D) 24 h.

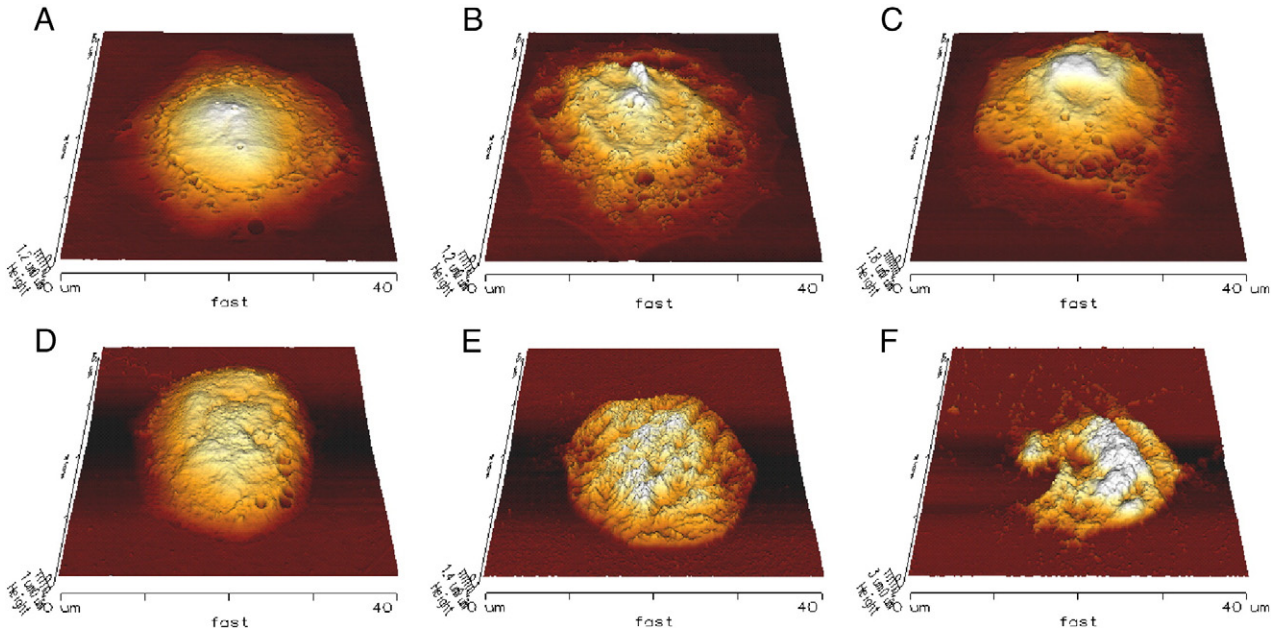

Fig. 7. AFM images (40×40 μm) of NCI-H460 and NCI-H520 treated with CB1a peptide. (A), (B) and (C) are of NCI-H460 cell and (D), (E) and (F) are of NCI-H520 cell treated with CB1a at 0 μM (A, D); 25 μM (B, E) and 50 μM (C, F), respectively. Incubation time is 30 min.

that of Dox. The Selectivity Index (SI) of CB1a (SI is a ratio of IC_{50} on normal lung cells to that of lung cancer cells) is larger than 15 on average, while, SI of Dox is mostly less than 1 (data not shown). Further evidence of CB1a's efficacy on lung cancer cells was obtained using MCTS modeling. Results indicated that CB1a had the ability to prevent lung cancer cells (NCI-H460) from forming tumor-like growths in test tubes. MCTS modeling gives guidance on the aggregation of cancer cells under gravity whereby cell–cell interactions are the main force allowing for cell aggregations to occur in solution. Under these circumstances, if cancer cell surfaces are not viable (compromised by physical attack from CB1a) they cannot interact with healthy cancer cell surfaces and aggregation is partially inhibited or cannot occur. This is shown in Fig. 4B and C for addition of CB1a at the time of seeding with cancer cells and 30 min prior to seeding, respectively. The example of adding CB1a to solution 30 min prior to seeding with cancer cells may tell us something of how this mechanism works. If cancer cell surfaces are more efficiently

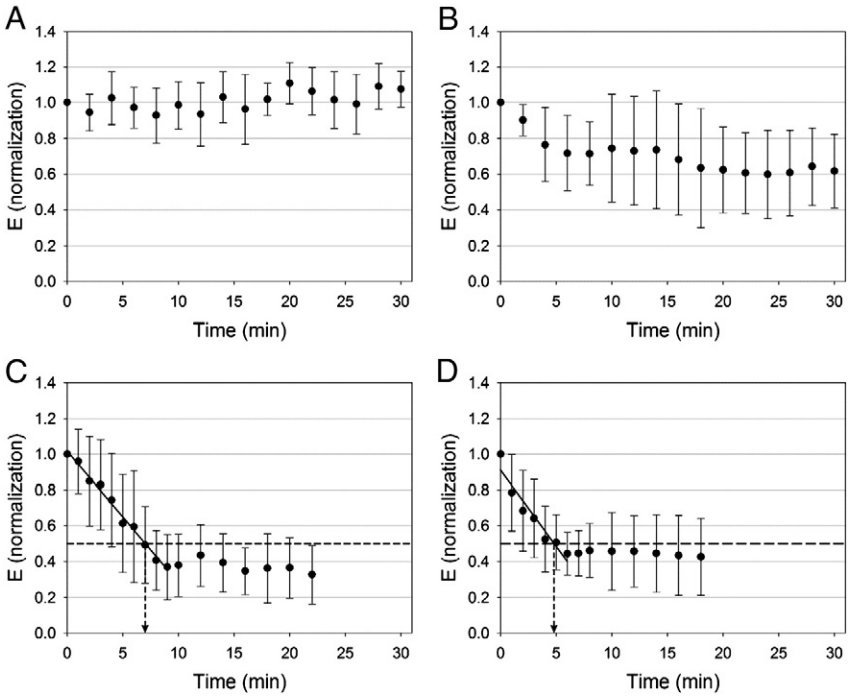

Fig. 8. Real time measurements of Young's modulus for single NCI-H460 cell. Cell was treated with CB1a at (A) 0 μM; (B) 12.5 μM; (C) 25 μM and (D) 50 μM within 30 min. Normalization of *E* shown in each figure is done for each data set at different times (0−30 min) divided by the original data at time zero. The results with standard deviations were done by using 10 representative cells per each AFM experiment. The symbolic arrows shown in figs. (C) and (D) indicated the IT_{50}s, which were 7.0 min and 4.8 min, respectively.

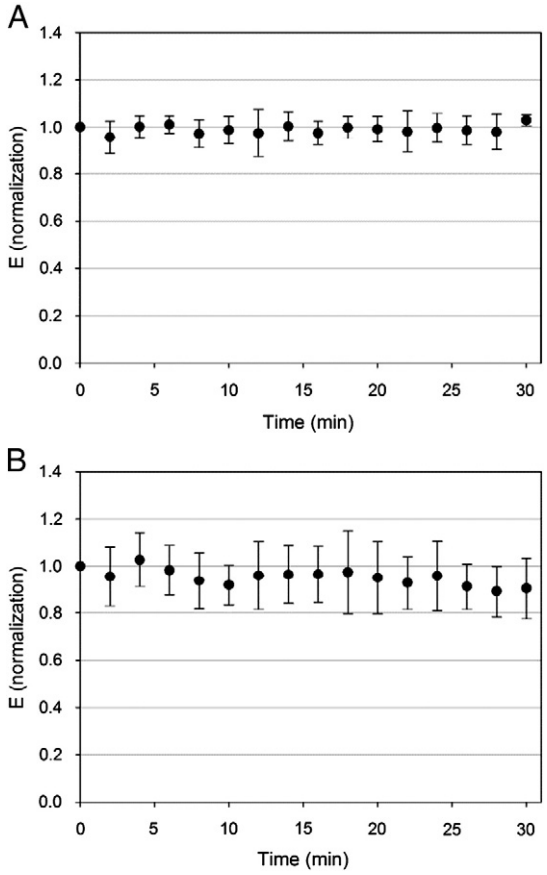

Fig. 9. Real time measurements of Young's modulus for single MRC-5 normal lung cell. Cell was treated with CB1a at (A) 5 μM and (B) 25 μM for no more than 30 min. The results with standard deviations were done by using 10 representative cells per each AFM experiment.

compromised by CB1a in solution then they have no time to interact with healthy cancer cells and aggregation is prevented (Fig. 4C). Dose dependence of CB1a on MCTS is further evidence of this (data not shown). These results could provide a future model for animal tests with peptide injections done in advance of the introduction of cancer cells. From a clinical point of view, if tolerated and deliverable, CB1a peptide could be used in early stage treatments or post surgery treatments when cancer cells are not so abundant. Furthermore, CB1a shows promise because of its high selectivity for cancer cells and low damage to normal lung cells (MRC-5, under CB1a (25 μM) at time = 24 h showed no obvious damage to cells, see Fig. 5F). CB1a's unique toxicity characteristics for normal tissue vs. cancerous tissue may be more favorable than those clinical drugs used for curing lung cancer.

The evidence of CB1a's efficacy in killing cancer cells *in vitro* made investigating the mechanism at a cellular level worthwhile. Current cancer drug Dox was again used as a reference compound. Morphological change of the cell surface during treatment with both drugs was investigated in real time using AFM. The study shows very different results for CB1a and Dox on normal lung cell, MRC-5. For Dox dosage of 18 μM, the normal cell's nucleus collapsed after an incubation time of 8 h. However, there was no evidence of damage to either the nucleus or cell as a whole under CB1a at 25 μM even after 24 h (see Fig. 5). Meanwhile, cancer cells NCI-H460 and NCI-H520 treated with CB1a at 25 μM showed considerable cellular breakdown after only 30 min (see Fig. 7). Clearly, CB1a is highly toxic to cancer cells, but has low toxicity toward normal cells. Consequently, we think CB1a has many favorable characteristics as a chemotherapeutic drug.

Further evidence of the mechanism by which CB1a kills cancer cells is provided by studying the changes in a cell's physical properties. Healthy cells have elastic properties. Under pressure (for example, from the external force applied by an AFM tip) a cell's shape becomes deformed but once the force is removed it will spring back to its original shape. However, if the cell surface is damaged (or membrane broken) by a drug like CB1a peptide, the cell loses its elasticity and this can be observed as a function of time. This work is the first of its kind to show cell degradation caused by CB1a and its direct relationship with elasticity change (or Young's modulus, *E*, change). The results confirmed that *E* reduced as a function of time when CB1a peptide was added to cancer cells. However, when CB1a was added to normal cells, *E* was almost a constant with time. This paper proposes that a new measure of drug efficacy IT_{50} be used in standard operating procedures (SOP) for future drug verification. IT_{50} is the interaction time between drug and target cell whereby *E* is reduced by 50%. Compared to the current standard IC_{50}, IT_{50} can be used as a measure at the single cell level over time whereas IC_{50} looks at bulk solutions. For example, for CB1a-treated NCI-H460 cancer cell, a reversed parabolic curve of *E vs.* time was obtained at 25 μM (see Fig. 8C) with IT_{50} of about 7.0 min. The IC_{50} of CB1a was 25 μM. Both IT_{50} (7.0 min) and IC_{50} (25 μM) can therefore be considered as cross verification for drug efficacy in *in vitro* investigations.

Dox uses a chemical pathway to kill cells through interaction with DNA by intercalation and inhibition of macromolecular biosynthesis [53,54]. The time needed to complete this inhibition action in cells leading cell to death for Dox may be longer (several hours) than CB1a requires to do physical damage to cancer cells (only about 20 min). The quickness with which CB1a kills cells may be explained by our previous results that CB1a peptide first binds with cancer cell surfaces through heparin-like binding and is then forced into the lipid membrane by hydrophilic and hydrophobic interactions with lipid heads and tails, respectively [39].

5. Conclusions

A customized anticancer peptide, CB1a, is shown to have high toxicity against lung cancer cells NCI-H460 and NCI-H520. It is also shown to be highly selective for these cells over normal lung cells, MRC-5. These two qualities suggest CB1a would make a good candidate for drug development. Additionally, the paper presents a new method for measuring drug efficacy IT_{50}—interaction time between drug and target cell whereby Young's Modulus *E* is reduced by 50%. For these experiments, CB1a has been shown to be potent against lung cancer cells with an IC_{50} of 25 μM and IT_{50} of 7.0 min. The cell death time was very quick and could be observed in real-time by AFM measurement. If compounds kill cells by a physical attach mechanism, IT_{50} may be an efficient method for verifying drug efficacy.

Acknowledgements

This work was in part supported by National Nano Device Laboratories and in part supported by the National Science Council of Taiwan.

Appendix A

AFM set-up for cell observation by microscope was shown below diagram. Sample showing cell surface and inside of cell (in light and dark reds, respectively) viewed by light microscope. AFM tip was properly adjusted to touch the cell. Upon scanning the cell by tip, the interaction force between the tip and cell surface causes a deflection. This deflection can be identified by a shift in the laser beam which is detectable by a quadrant photodiode. During data processing, all electric signals are transformed into either height (μm) or force (N) and both a topographic image and force relationship curve could be obtained (see right-side figures).

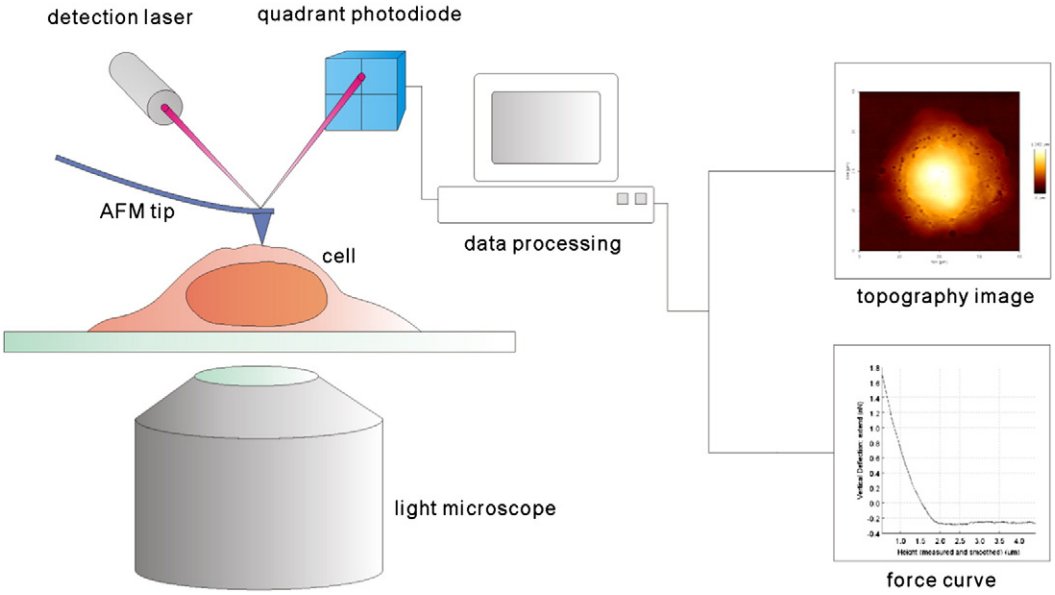

References

[1] R.E. Hancock, D.S. Chapple, Peptide antibiotics, Antimicrob. Agents Chemother. 43 (1999) 1317–1323.
[2] R.I. Lehrer, T. Ganz, Antimicrobial peptides in mammalian and insect host defence, Curr. Opin. Immunol. 11 (1999) 23–27.
[3] C.A. Olsen, H.L. Ziegler, H.M. Nielsen, N. Frimodt-Møller, J.W. Jaroszewski, H. Franzyk, Antimicrobial, hemolytic, and cytotoxic activities of β-peptoid–peptide hybrid oligomers: improved properties compared to natural amps, Chembiochem 11 (2010) 1356–1360.
[4] F. Costa, I.F. Carvalho, R.C. Montelaro, P. Gomes, M.C.L. Martins, Covalent immobilization of antimicrobial peptides (AMPs) onto biomaterial surfaces, Acta Biomater. 7 (2011) 1431–1440.
[5] D. Zweytick, G. Deutsch, J. Andra, S.E. Blondelle, E. Vollmer, R. Jerala, K. Lohner, Studies on lactoferricin-derived Escherichia coli membrane-active peptides reveal differences in the mechanism of N-acylated versus nonacylated peptides, J. Biol. Chem. 286 (2011) 21266–21276.
[6] H. Steiner, D. Hultmark, A. Engstrom, H. Bennich, H.G. Boman, Sequence and specificity of two antibacterial proteins involved in insect immunity, Nature 292 (1981) 246–248.
[7] H.M. Chen, W. Wang, D. Smith, S.C. Chan, Effects of the anti-bacterial peptide cecropin B and its analogs, cecropins B-1 and B-2, on liposomes, bacteria, and cancer cells, Biochim. Biophys. Acta 1336 (1997) 171–179.
[8] X. Han, L. Soblosky, M. Slutsky, C.M. Mello, Z. Chen, Solvent effect and time-dependent behavior of C-terminus-cysteine-modified cecropin P1 chemically immobilized on a polymer surface, Langmuir 27 (2011) 7042–7051.
[9] M. Zasloff, Magainins, a class of antimicrobial peptides from *Xenopus* skin: isolation, characterization of two active forms, and partial cDNA sequence of a precursor, Proc. Natl. Acad. Sci. U. S. A. 84 (1987) 5449–5453.
[10] Y. Ohsaki, A.F. Gazdar, H.C. Chen, B.E. Johnson, Antitumor activity of magainin analogues against human lung cancer cell lines, Cancer Res. 52 (1992) 3534–3538.
[11] M.A. Baker, W.L. Maloy, M. Zasloff, L.S. Jacob, Anticancer efficacy of Magainin2 and analogue peptides, Cancer Res. 53 (1993) 3052–3057.
[12] A. Zairi, F. Tangy, K. Bouassida, K. Hani, Dermaseptins and magainins: antimicrobial peptides from frogs' skin-new sources for a promising spermicides microbicides—a mini review, J. Biomed. Biotechnol. 2009 (2009) 1–8.
[13] A. Ramamoorthy, S. Thennarasu, D.-K. Lee, A. Tan, L. Maloy, Solid-state NMR investigation of the membrane-disrupting mechanism of antimicrobial peptides MSI-78 and MSI-594 derived from magainin 2 and melittin, Biophy. J. 91 (2006) 206–216.
[14] L.M. Gottler, A. Ramamoorthy, Structure, membrane orientation, mechanism, and function of pexiganan—a highly potent antimicrobial peptide designed from magainin, Biochim. Biophys. Acta, Biomembr. 1788 (2009) 1680–1686.
[15] S.V. Sharma, Melittin resistance: a counterselection for ras transformation, Oncogene 7 (1992) 193–201.
[16] S.V. Sharma, Melittin-induced hyperactivation of phospholipase A2 activity and calcium influx in ras-transformed cells, Oncogene 8 (1993) 939–947.
[17] A. Niemz, D.A. Tirrell, Self-association and membrane-binding behavior of melittins containing trifluoroleucine, J. Am. Chem. Soc. 123 (2001) 7407–7413.
[18] M. Frohm, B. Agerberth, G. Ahangari, M. Stahle-Backdahl, S. Liden, H. Wigzell, G.H. Gudmundsson, The expression of the gene coding for the antibacterial peptide LL-37 is induced in human keratinocytes during inflammatory disorders, J. Biol. Chem. 272 (1997) 15258–15263.
[19] J. Johansson, G.H. Gudmundsson, M.E. Rottenberg, K.D. Berndt, B. Agerberth, Conformation-dependent antibacterial activity of the naturally occurring human peptide LL-37, J. Biol. Chem. 273 (1998) 3718–3724.
[20] F. Porcelli, R. Verardi, L. Shi, K.A. Henzler-Wildman, A. Ramamoorthy, G. Veglia, NMR structure of the cathelicidin-derived human antimicrobial peptide LL-37 in dodecylphosphocholine micelles, Biochemistry 47 (2008) 5565–5572.
[21] J.-Y. Moon, K.A. Henzler-Wildman, A. Ramamoorthy, Expression and purification of a recombinant LL-37 from *Escherichia coli*, Biochim. Biophys. Acta 1758 (2006) 1351–1358.
[22] U.H.N. Dürr, U.S. Sudheendra, A. Ramamoorthy, LL-37, the only human member of the cathelicidin family of antimicrobial peptides, Biochim. Biophys. Acta 1758 (2006) 1408–1425.
[23] D.W. Hoskin, A. Ramamoorthy, Studies on anticancer activities of antimicrobial peptides, Biochim. Biophys. Acta 1778 (2008) 357–375.
[24] N. Papo, Y. Shai, Host defense peptides as new weapons in cancer treatment, Cell. Mol. Life Sci. 62 (2005) 784–790.
[25] L. Steinstraesser, J. Hauk, C. Schubert, S. Al-Benna, I. Stricker, H. Hatt, Y. Shai, H.-U. Steinau, F. Jacobsen, Suppression of soft tissue sarcoma growth by a host defense-like lytic peptide, PLoS One 6 (2011) e18321.
[26] V. Dhople, A. Krukemeyer, A. Ramamoorthy, The human beta-defensin-3, an antibacterial peptide with multiple biological functions, Biochim. Biophys. Acta 1758 (2006) 1499–1512.
[27] S. Bhattacharjya, A. Ramamoorthy, Multifunctional host defense peptides: functional and mechanistic insights from NMR structures of potent antimicrobial peptides, FEBS J. 276 (2009) 6465–6473.
[28] A. Ramamoorthy, Beyond NMR spectra of antimicrobial peptides: dynamical images at atomic resolution and functional insights, Solid State Nucl. Magn. Res. 35 (2009) 201–207.
[29] E. Sarafraz-Yazdi, W.B. Bowne, V. Adler, K.A. Sookraj, V. Wu, V. Shteyler, H. Patel, W. Oxbury, P. Brandt-Rauf, M.E. Zenilman, J. Michl, M.R. Pincus, Anticancer peptide PNC-27 adopts an HDM-2-binding conformation and kills cancer cells by binding to HDM-2 in their membranes, Proc. Natl. Acad. Sci. U. S. A. 107 (2010) 1918–1923.
[30] S. Riedl, D. Zweytick, K. Lohner, Membrane-active host defense peptides—challenges and perspectives for the development of novel anticancer drugs, Chem. Phys. Lipids 164 (2011) 766–781.
[31] N.R. Soman, S.L. Baldwin, G. Hu, J.N. Marsh, G.M. Lanza, J.E. Heuser, J.M. Arbeit, S.A. Wickline, P.H. Schlesinger, Molecularly targeted nanocarriers deliver the cytolytic peptide melittin specifically to tumor cells in mice, reducing tumor growth, J. Clin. Invest. 119 (2009) 2830–2842.
[32] P. van Hofsten, I. Faye, K. Kockum, J.Y. Lee, K.G. Xanthopoulos, I.A. Boman, H.G. Boman, A. Engstrom, D. Andreu, R.B. Merrifield, Molecular cloning, cDNA sequencing, and chemical synthesis of cecropin B from *Hyalophora cecropia*, Proc. Natl. Acad. Sci. U. S. A. 82 (1985) 2240–2243.
[33] W. Wang, D.K. Smith, H.M. Chen, The effect of pH on the structure, binding and model membrane lysis by cecropin B and analogs, Biochim. Biophys. Acta 1473 (1999) 418–430.
[34] W. Wang, D.K. Smith, K. Moulding, H.M. Chen, The dependence of membrane permeability by the antibacterial peptide cecropin B and its analogs, CB-1 and CB-3, on liposomes of different composition, J. Biol. Chem. 273 (1998) 27438–27448.
[35] H.M. Chen, A.H. Clayton, W. Wang, W.H. Sawyer, Kinetics of membrane lysis by custom lytic peptides and peptide orientations in membrane, Eur. J. Biochem. 268 (2001) 1659–1669.

[36] H.M. Chen, K.W. Leung, N.N. Thakur, A. Tan, R.W. Jack, Distinguishing between different pathways of bilayer disruption by the related antimicrobial peptides cecropin B, B1 and B3, Eur. J. Biochem. 270 (2003) 911–920.
[37] S. Srisailam, A.I. Arunkumar, W. Wang, C. Yu, H.M. Chen, Conformational study of a custom antibacterial peptide cecropin B1: implications of the lytic activity, Biochim. Biophys. Acta 1479 (2000) 275–285.
[38] S. Srisailam, T.K. Kumar, A.I. Arunkumar, K.W. Leung, C. Yu, H.M. Chen, Crumpled structure of the custom hydrophobic lytic peptide cecropin B3, Eur. J. Biochem. 268 (2001) 4278–4284.
[39] J.M. Wu, P.S. Jan, H.C. Yu, H.Y. Haung, H.J. Fang, Y.I. Chang, J.W. Cheng, H.M. Chen, Structure and function of a custom anticancer peptide, CB1a, Peptides 30 (2009) 839–848.
[40] D.P. Tieleman, I.H. Shrivastava, M.R. Ulmschneider, M.S. Sansom, Proline-induced hinges in transmembrane helices: possible roles in ion channel gating, Proteins 44 (2001) 63–72.
[41] D.K. Chang, S.F. Cheng, V.D. Trivedi, K.L. Lin, Proline affects oligomerization of a coiled coil by inducing a kink in a long helix, J. Struct. Biol. 128 (1999) 270–279.
[42] S.E. Cross, Y.S. Jin, J. Rao, J.K. Gimzewski, Nanomechanical analysis of cells from cancer patients, Nat. Nanotechnol. 2 (2007) 780–783.
[43] Q.S. Li, G.Y. Lee, C.N. Ong, C.T. Lim, AFM indentation study of breast cancer cells, Biochem. Biophys. Res. Commun. 374 (2008) 609–613.
[44] C. Rotsch, K. Jacobson, M. Radmacher, Dimensional and mechanical dynamics of active and stable edges in motile fibroblasts investigated by using atomic force microscopy, Proc. Natl. Acad. Sci. U. S. A. 96 (1999) 921–926.
[45] C. Rotsch, M. Radmacher, Drug-induced changes of cytoskeletal structure and mechanics in fibroblasts: an atomic force microscopy study, Biophys. J. 78 (2000) 520–535.
[46] M.J. Rosenbluth, W.A. Lam, D.A. Fletcher, Force microscopy of nonadherent cells: a comparison of leukemia cell deformability, Biophys. J. 90 (2006) 2994–3003.
[47] W.A. Lam, M.J. Rosenbluth, D.A. Fletcher, Chemotherapy exposure increases leukemia cell stiffness, Blood 109 (2007) 3505–3508.
[48] J.C. Martens, M. Radmacher, Softening of the actin cytoskeleton by inhibition of myosin II, Pflugers Arch. 456 (2008) 95–100.
[49] C. Callies, J. Fels, I. Liashkovich, K. Kliche, P. Jeggle, K. Kusche-Vihrog, H. Oberleithner, Membrane potential depolarization decreases the stiffness of vascular endothelial cells, J. Cell Sci. 124 (2011) 1936–1942.
[50] R.B. Merrifield, Solid phase peptide synthesis. I. The synthesis of a tetrapeptide, J. Am. Chem. Soc. 85 (1963) 2149–2154.
[51] D. Del Duca, T. Werbowetski, R. Del Maestro, Spheroid preparation from hanging drops: characterization of a model of brain tumor invasion, J Neurooncol 67 (2004) 295–303.
[52] T.G. Kuznetsova, M.N. Starodubtseva, N.I. Yegorenkov, S.A. Chizhik, R.I. Zhdanov, Atomic force microscopy probing of cell elasticity, Micron 38 (2007) 824–833.
[53] R.L. Momparler, M. Karon, S.E. Siegel, F. Avila, Effect of adriamycin on DNA, RNA, and protein synthesis in cell-free systems and intact cells, Cancer Res. 36 (1976) 2891–2895.
[54] F.A. Fornari, J.K. Randolph, J.C. Yalowich, M.K. Ritke, D.A. Gewirtz, Interference by doxorubicin with DNA unwinding in MCF-7 breast tumor cells, Mol. Pharmacol. 45 (1994) 649–656.